

# Searches for UHE neutrinos and upward-going showers at the Pierre Auger Observatory

---

**Jaime Alvarez-Muñiz<sup>a,\*</sup> for the Pierre Auger Collaboration<sup>b</sup>**

<sup>a</sup>*Instituto Galego de Física de Altas Enerxías (IGFAE), Universidade de Santiago de Compostela  
15782 Santiago de Compostela, Spain*

<sup>b</sup>*Observatorio Pierre Auger*

*Av. San Martín Norte 304, 5613 Malargüe, Argentina*

*Full author list: [https://www.auger.org/archive/authors\\_2024\\_11.html](https://www.auger.org/archive/authors_2024_11.html)*

*E-mail: [spokespersons@auger.org](mailto:spokespersons@auger.org)*

The Pierre Auger Observatory, as a key actor in multi-messenger astronomy, is playing a crucial role in searching for and following-up cosmic phenomena across different channels. Data from the Observatory have been utilized for nearly 20 years to search for showers induced by Ultra-High-Energy (UHE) neutrinos with energies exceeding 0.1 EeV. Neutrino-induced showers at high zenith angles are likely to develop deep in the atmosphere, resulting in a significant electromagnetic component that distinguishes them from the cosmic-ray background. This enables the identification of candidate events from both neutrinos interacting in the atmosphere and Earth-skimming  $\tau$  neutrinos. Searches have been conducted for both diffuse and point sources using data collected by the Surface Detector, a large array of over 1660 water-Cherenkov stations spread over an area of 3000 km<sup>2</sup>. Additionally, the Fluorescence Detector consisting of 27 telescopes has been employed to search for upward-developing air showers, as predicted by several interpretations of the 'anomalous' events detected by the ANITA detector. In this contribution, we summarize the main results obtained in these searches and discuss their astrophysical implications.

*7th International Symposium on Ultra High Energy Cosmic Rays (UHECR2024)  
17-21 November 2024  
Malargüe, Mendoza, Argentina*

---

\*Speaker

## 1. Introduction

The origin, nature, and production mechanisms of ultra-high-energy cosmic rays (UHECRs) with energies exceeding  $1 \text{ EeV} = 10^{18} \text{ eV}$  remain some of the long-standing questions in astroparticle physics. All models of UHECR production predict the generation of UHE neutrinos as a consequence of the decay of charged pions, which are produced in interactions of UHECRs within the sources themselves (“astrophysical” neutrinos) and/or during their propagation through background radiation fields (“cosmogenic” neutrinos).

The Pierre Auger Observatory [1], near the town of Malargüe in Argentina is the largest UHECR observatory in the world. One of its key features is its hybrid design, which integrates a Surface Detector array (SD) with a Fluorescence Detector (FD). The so-called SD1500 array, part of the SD, consists of  $\sim 1660$  water-Cherenkov detectors in a triangular grid with 1500 m distance between them covering an area of about  $3000 \text{ km}^2$ . The atmosphere above the array is monitored by 27 fluorescence telescopes, distributed across four sites at its borders. The SD samples the lateral shower profile at ground level, i.e., the distribution of secondary particles as a function of their distance from the shower axis, operating with a duty cycle of  $\sim 100\%$ . In contrast, the FD records the longitudinal shower development in the atmosphere above the SD, but it can only function on clear, moonless nights, limiting its duty cycle to about  $\sim 15\%$ .

The Antarctic Impulsive Transient Antenna (ANITA) on long-duration NASA balloons at 30–39 km above Antarctica has detected radio pulses consistent with coherent emissions from UHECR-air showers after the radio waves reflect on the Antarctic ice. Two *anomalous* pulses have also been observed from below the horizon [2, 3]. These are not compatible with being reflected UHECR, suggesting that the emission could be from upward-developing air showers, possibly from  $\tau$ -lepton decays produced by UHE  $\tau$ -neutrinos interacting below the surface of the Earth. However, the observed pulse directions and estimated energy of the events imply the neutrinos would undergo significant attenuation in the Earth, requiring a flux that should be detectable by IceCube and the Pierre Auger Observatory [4–6].

In this contribution, we present the analysis of data collected with the SD1500 of Auger, focusing on the search for UHE neutrinos, and of data collected with the FD, in the search for upward-developing air showers.

## 2. Search for UHE neutrinos

The main challenge in searching for UHE neutrinos is differentiating air showers triggered by neutrinos from those produced by the much more abundant background of primary protons and heavier nuclei in cosmic rays. These particles initiate air showers at high altitudes as they enter the atmosphere. At large zenith angles  $\theta \gtrsim 60^\circ$ , the electromagnetic component is almost entirely absorbed in the atmosphere, and, as a first approximation, only muons reach the surface of the Earth. Neutrinos, which can interact anywhere in the atmosphere due to their eight orders of magnitude smaller cross section, can initiate air showers closer to the ground, allowing the electromagnetic component to be detected even in the quasi-horizontal directions. This creates a distinctive signature that can effectively be used to identify UHE neutrino-induced showers using the SD. Another search channel is provided by Earth-skimming  $\tau$  neutrinos, which can interact

within the Earth's crust, producing a  $\tau$  lepton that enters the atmosphere from below, creating a slightly upward-going air shower near the ground that can trigger the SD. UHE neutrino searches with the SD1500 at the Pierre Auger Observatory focus on detecting these signatures. For that purpose, the analysis is divided by zenith angle into two categories: the Earth-skimming channel (ES, zenith angles between  $90^\circ$  and  $95^\circ$ ) and the down-going channel (DG, zenith angles between  $60^\circ$  and  $90^\circ$ ). The DG channel is split into two sub-channels based first on the zenith angle, namely, Downward-Going Low-angle or DGL with  $\theta \in (58.5^\circ, 76.5^\circ)$ , and Downward-Going High-angle or DGH with  $\theta \in (75^\circ, 90^\circ)$ .

To separate the electromagnetic and muonic components of the shower, variables related to the spread of the 25 ns-binned signal time traces are used. The separation is based on the fact that electrons in the shower suffer multiple scattering and are expected to arrive more spread in time than muons that travel almost in straight lines to the detector inducing shorter signals. In the ES channel, the average area-over-peak  $\langle \text{AoP} \rangle$ , which is the ratio of the time trace integral in an SD station to its peak value, averaged over all triggered stations in an SD event, is used as the key discriminating observable based on this idea [7]. In the DG channel, the analysis is also based on AoP values. However, in this case, additional observables are constructed from the individual AoP values of the stations, and these are then combined in a Fisher discriminant analysis [7].

The search for UHE neutrinos in Auger is based on a *blind* procedure where a small fraction of data (*burn sample*) is used to establish a set of cuts, first to select inclined showers, and then to identify those with a large electromagnetic component at ground, indicative of a deep downward-going shower in the atmosphere or an Earth-Skimming event. The final cut on the value of  $\langle \text{AoP} \rangle$  in the ES channel or the Fisher value in the DG channels above which an event would be regarded as a neutrino candidate, are chosen exploiting the burn sample by requiring less than 1 expected background event in several decades of data taking (depending on the channel). After that, the same set of cuts is applied to the full data in the period from January 1, 2004, to December 31, 2021. An example of the result of unblinding in the ES channel is shown in the left panel of Fig. 1.

Since no neutrino events were observed in any of the search channels, upper limits on the diffuse neutrino flux are established by combining the results from all search channels. Assuming a (single flavor) neutrino flux of the form  $\phi = k \times E_\nu^{-2}$ , an upper limit on the normalization  $k$  for the energy range between  $10^{17}$  eV and  $2.5 \times 10^{19}$  eV is found to be  $3.5 \times 10^{-9}$  GeV cm $^{-2}$  s $^{-1}$  sr $^{-1}$ . Upper limits can also be determined for energy bins with a width of 0.5 in  $\log_{10}(E_\nu/\text{eV})$ , which provides a useful way to describe the energy dependence of the sensitivity. The Pierre Auger Observatory reaches its best sensitivity around  $10^{18}$  eV. The upper limits are displayed in the right panel of Fig. 1, along with corresponding upper limits from IceCube and ANITA, and the expected neutrino fluxes under various theoretical models and assumptions. These results allow us to constrain different classes of models for neutrino production, both cosmogenic and astrophysical. Specifically, cosmogenic models that assume a pure-proton composition and a strong source evolution with redshift are significantly constrained and even ruled out due to the lack of neutrino detections. Cosmogenic models assuming the mixed composition observed in Auger data predict event rates that are typically one order of magnitude below the sensitivity of the current Auger configuration. Some models of production of astrophysical neutrinos in Active Galactic Nuclei are ruled out by Auger data, while others assuming BL-Lacs, magnetars or starburst galaxies are started to be constrained.

The absence of neutrino candidates in Auger data also allows us to put constraints on point-like

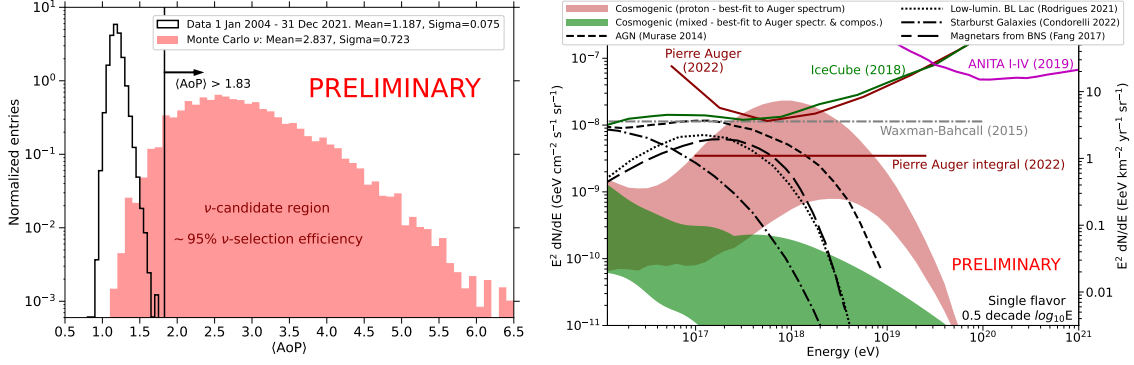


**Figure 1:** Left: Results of the unblinding for the ES search channel based on the discrimination variable  $\langle \text{AoP} \rangle$  (see text). Black histogram: data from January 1, 2004, to December 31, 2021. Red-filled histogram: neutrino simulations. A vertical line indicates the value of  $\langle \text{AoP} \rangle > 1.83$  above which an event would be regarded as a neutrino candidate. Right: Upper limits on the diffuse flux of neutrinos, both integral (straight solid line) as well as differential (curved solid line). Also shown are upper limits from IceCube and ANITA and the expected neutrino fluxes under different theoretical assumptions and scenarios, including ones based on Auger data (cf. [8]). For details and references see [7].

sources of UHE neutrinos, both transient and continuous, across a large fraction of the sky from near the equatorial South Pole to declination  $\delta \sim +60^\circ$ , with the largest sensitivity at declinations around  $\delta \sim -50^\circ$  and  $\delta \sim +55^\circ$  due to the ES channel [9]. With an instantaneous field-of-view of  $\approx 30\%$  of the sky as shown in the left panel of Fig. 2 with Auger data we have been able to put unmatched constraints on the UHE neutrino flux from the coalescence of the binary system GW170817 detected in gravitational waves and across the electromagnetic spectrum [10], as well as from the blazar TXS 0506+056 [11], the first extragalactic source of high-energy neutrinos identified by the IceCube Observatory. These capabilities position the Auger SD as a crucial and complementary detector in multi-messenger astronomy at UHE.

### 3. Search for upward-going showers

The two anomalous events detected in the ANITA I [2] and ANITA III [3] flights, have generated a great deal of interest, especially after Standard Model explanations attributing them to upward-going  $\nu_\tau$  have been largely ruled out [4–6]. Alternative explanations based on physics beyond the Standard Model have been proposed, speculating on the existence of new particles that induce upward-going showers, e.g. [12–14]. To investigate this possibility, we have conducted a dedicated search for upward-going air showers in data collected with the FD of the Pierre Auger Observatory [15].

The energy of the anomalous showers depends on the altitude at which the shower starts in the atmosphere. With simulated showers at altitudes of  $0 < h < 9$  km the estimated minimum energy for the ANITA I (ANITA III) anomalous event with elevation angle  $27.4^\circ$  ( $35.0^\circ$ ) corresponding to zenith angle  $\theta = 116.7^\circ$  ( $\theta = 124.5^\circ$ ) at the intercept of the trajectory with the ice cap, is around 0.2 EeV (0.15 EeV) for showers starting at  $h \sim 5$  km ( $h > 5$  km) [4]. The search for upward-going showers with FD has been restricted to zenith angles exceeding  $\theta = 110^\circ$  (elevation  $> 20^\circ$ ) and

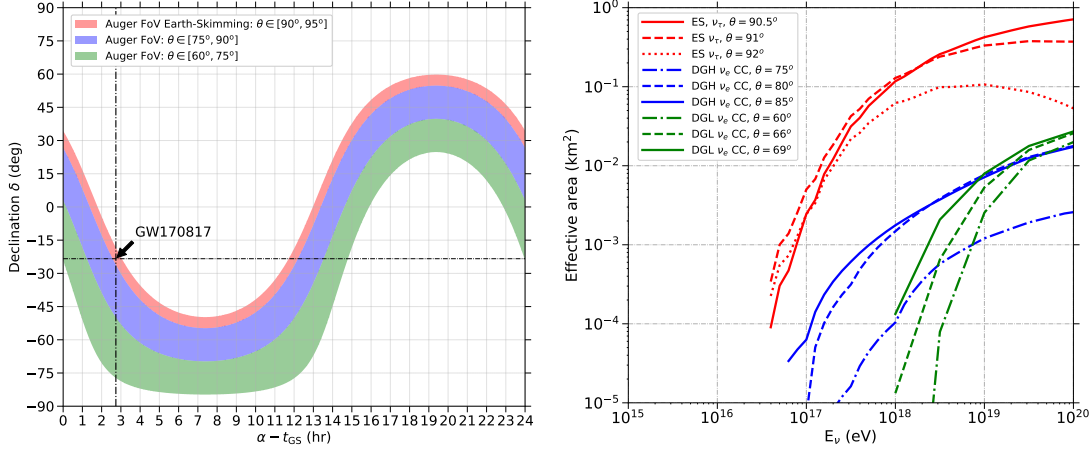


**Figure 2:** Left: Instantaneous field-of-view of the Pierre Auger Observatory for the ES (red band) and DG (blue and green). The declination is plotted as a function of  $\alpha - t_{GS}$  where  $t_{GS}$  is the Greenwich Sidereal Time converted to the mean longitude of the Observatory. The position of the binary neutron star GW170817 at the instant of coalescence overlapping with the ES fov is indicated with an arrow. Right: Instantaneous effective areas of the Auger Observatory for ES (red lines), and DG (blue and green) channels as a function of neutrino energy for several zenith angles.

energies  $E > 0.1$  EeV. For showers with  $\theta > 110^\circ$ , only FD data is used, as these events do not trigger the SD.

The standard FD reconstruction of air shower properties involves a two-stage process: a geometrical reconstruction using timing information from triggered pixels in the FD camera, followed by an energy deposition reconstruction using the Gaisser-Hillas profile. An alternative Global Fit (GF) method uses all available pixel data for a more accurate reconstruction [16]. In both cases, upward and downward modes are distinguished based on the time sequence of the active pixels. In the absence of SD information ambiguities can arise. For instance, downward-going quasi-horizontal events can be mis-reconstructed as upward-going, and showers whose core falls behind the FD detector developing above it can also induce an upward-going track in the FD camera. Also, showers with  $\theta > 90^\circ$  relative to zenith at the center of the SD array and that do not intercept the surface of the Earth form part of the background.

A different kind of background present in the data is due to laser pulses emitted in the upward direction at a rate of about 150 Hz. These are used to monitor the atmospheric quality and FD performance. While most laser events can be identified and vetoed, a small fraction (0.01%) is not properly labeled. A burn sample of 10% of the FD data has been used to identify and establish a set of selection cuts to clean these events based on their frequency and location over the SD.

A blind analysis strategy has also been followed in this analysis to establish the selection of upward-going showers, using simulations and the burn sample, before applying the selection to the full data set in the period from January 1, 2004, to December 31, 2018. Simulations of UHECR-induced showers (background) and upward-going showers (signal) have been produced using CONEX. The background simulations included showers of proton, helium, nitrogen, and iron primaries over the energy range 0.1–100 EeV. The showers were isotropically injected, with zenith

angles from  $0^\circ$  to  $100^\circ$ , and the energy distribution was weighted to match the measured UHECR spectrum [17]. For signal simulation, upward-going proton showers were produced in the 0.03–10 EeV range, an example is shown in Fig. 3. Showers were simulated to develop at altitudes between  $h = 0$  and 9 km, and the impact points were sampled in a  $100 \times 100 \text{ km}^2$  area centered on the SD array.

A series of cuts studied with simulations are applied sequentially, first to the 10% burn sample for verification before being blindly applied to the full FD dataset of  $7.6 \times 10^6$  events. In the first step, laser cuts are applied, and only events in time periods with clean atmospheric conditions and low cloud coverage, as well as having at least six camera pixels for time-geometry fitting are used. Of these, only those reconstructed as upward-going using a simple time-geometry fit are kept. The GF reconstruction is then applied to verify the consistency of pixel intensities with a shower-like  $dE/dX$  profile, eliminating events dominated by Cherenkov light that are often mis-reconstructed as upward-going in the simple time fit. After this step, the GF is also applied to the remaining events in downward mode, and it is found that most events are compatible with both upward and downward reconstructions. After applying quality cuts on atmospheric slant depth and shower maximum, a cut on  $\theta > 110^\circ$ , and further cuts based on reconstruction quality, only 255 events survive.

At this stage, and to discriminate between upward-going showers (signal) and cosmic-ray events (background), a discrimination variable was introduced based on the logarithmic likelihood ratio of upward and downward reconstructions,  $L_{\text{up}}/L_{\text{down}}$ , and defined as:

$$l = \frac{\arctan \left[ \ln \left( \frac{\max(L_{\text{up}}, L_{\text{down}})}{L_{\text{down}}} \right) \cdot \zeta \right]}{\pi/2}. \quad (1)$$

The variable  $l$  ranges from 0 to 1, where larger values indicate stronger upward-going likelihoods. If  $L_{\text{down}} > L_{\text{up}}$ ,  $l$  is 0, and if the event can only be reconstructed upward,  $l = 1$ . The parameter  $\zeta$  is chosen to evenly distribute the signal events over the range  $[0,1]$  for events with  $L_{\text{up}} > L_{\text{down}}$ . A final cut,  $l > l_c$ , is applied to optimize the background-signal discrimination. The optimal value of  $l_c = 0.55$  is found by minimizing the upper limit on the integral flux of upward-going showers, with the background expected at  $n_{\text{bkg}} = 0.27 \pm 0.12$  events.

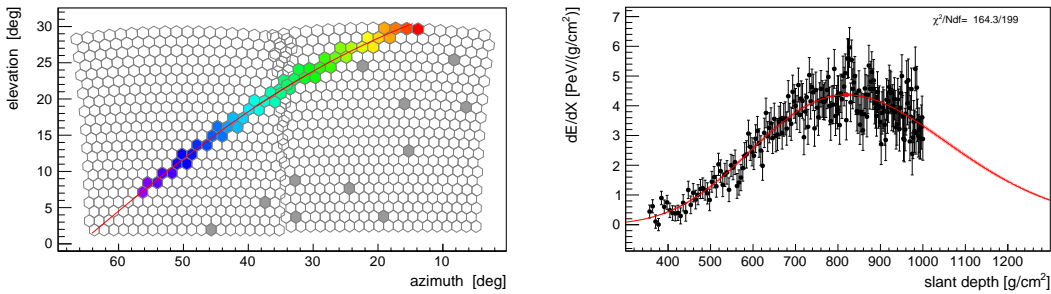


**Figure 3:** Example of a simulated and reconstructed upward-going shower in the FD. Left: Triggered pixels of the FD camera showing the earliest one in purple and the last one in red. Right: Best fit to a Gaisser-Hillas profile of the energy deposit in the atmosphere. The  $\chi^2$  value of the fit is indicated.

After applying the selection cuts to the full data set, one candidate event is found, having  $l = 1$  (only upward-going reconstruction allowed), triggering only six pixels and with a moderate



reconstruction quality [15]. This event is consistent with background expectations, and in fact similar events have been obtained with Monte Carlo simulations of background UHECR.

Using the same selection criteria on signal simulations, the effective area and exposure of the FD for upward-going showers is calculated as a function of energy and starting altitude. The exposure of ANITA I and III was obtained analytically following a similar procedure to that used with numerical calculations in [4]. As a result, the exposure of the FD of the Pierre Auger Observatory is a factor between 2 and 2000 larger than that of ANITA in the zenith angle range  $\theta \in [110^\circ, 130^\circ]$  [15].

Assuming that the ANITA events are indeed due to upward-going showers, the measured flux can be obtained to account for 1 event in each ANITA flight. When this flux is folded with the exposure of the FD of the Pierre Auger Observatory, the expected number of events would be between  $\approx 10$  and  $\approx 70$ , depending on the assumed behaviour of the flux with energy and on the assumptions on the distribution of altitudes of shower generation, either uniform in altitude or compatible with that expected from  $\tau$  decays. Given only one observed event in data compatible with background, this suggests that upward-going showers cannot account for the anomalous pulses detected by ANITA that remain unexplained.

The exposures of ANITA and the FD of the Pierre Auger Observatory differ significantly in their dependence on shower altitude. The FD is most sensitive to low-altitude showers that are closer to the detector when compared to ANITA, and is unlikely to detect showers that start at higher altitudes or have unusual shower profiles, offering a possible explanation for the absence of signal events in data collected at the Auger Observatory. However, these possibilities would contradict expectations from known particle decays and interactions.

#### 4. Conclusions

The search for UHE neutrinos using the Surface Detector (SD) of the Pierre Auger Observatory has yielded no candidates from January 1, 2004, to December 31, 2021. As a result, competitive limits have been set on diffuse fluxes, with the largest sensitivity around 1 EeV, and with pure proton cosmogenic neutrino models significantly constrained. The Auger Observatory also possesses large instantaneous sensitivity to bursting sources in the Earth-Skimming Field of View, positioning it as a key player in multimessenger astronomy at UHE. Ongoing follow-up efforts include searches for signals from binary neutron star mergers (BNS), binary black hole mergers (BBH) [18], and other flaring sources.

In parallel, searches for upward-going showers using the Fluorescence Detector (FD) of the Pierre Auger Observatory, motivated by the anomalous events detected by the ANITA experiment, have been conducted. Between January 1, 2004 and December 31, 2018, only one event was found in data, which was consistent with background expectations. Given the significantly larger exposure of the FD of the Pierre Auger Observatory compared to ANITA, at least 10 upward-going events would have been expected under various assumptions of the energy flux slope and decay height distribution. The observation of only one event that is compatible with background dismisses a shower origin for the ANITA anomalous events, leaving the question on their origin still unresolved.

## References

- [1] A. Aab et al. [Pierre Auger Coll.], *Nucl. Instrum. Meth. A* **798** (2015) 172 [[arXiv:1502.01323](#)].
- [2] P.W. Gorham et al. [ANITA Coll.], *Phys. Rev. Lett.* **117** (2016) 071101 [[arXiv:1603.05218](#)].
- [3] P.W. Gorham et al. [ANITA Coll.], *Phys. Rev. Lett.* **121** (2018) 161102 [[arXiv:1803.05088](#)].
- [4] A. Romero-Wolf, S. A. Wissel, H. Schoorlemmer, W. R. Carvalho, J. Alvarez-Muñiz, E. Zas, P. Allison, O. Banerjee, L. Batten and J. J. Beatty, *et al. Phys. Rev. D* **99** (2019) 063011 [[arXiv:1811.07261](#)].
- [5] I. Safa, A. Pizzuto, C. A. Argüelles, F. Halzen, R. Hussain, A. Kheirandish and J. Vandenbroucke, *JCAP* **01** (2019) 012 [[arXiv:1909.10487](#)].
- [6] S. Chipman, R. Diesing, M. H. Reno and I. Sarcevic, *Phys. Rev. D* **100** (2019) 063011 [[arXiv:1906.11736](#)].
- [7] A. Aab et al. [Pierre Auger Coll.], *JCAP* **10** (2019) 022 [[arXiv:1906.07422](#)].
- [8] C. Petrucci [Pierre Auger Coll.], *PoS (ICRC 2023)* (2023) 1520.
- [9] A. Aab *et al.* [Pierre Auger], *JCAP* **11** (2019) 004 [[arXiv:1906.07419](#)].
- [10] A. Albert et al. [ANTARES, IceCube, Pierre Auger, LIGO Scientific, Virgo Colls.], *Astrophys. J. Lett.* **850** (2017) L35 [[arXiv:1710.05839](#)].
- [11] A. Aab *et al.* [Pierre Auger], *Astrophys. J.* **902** (2020) 105 [[arXiv:2010.10953](#)].
- [12] D. B. Fox, S. Sigurdsson, S. Shandera, P. Mészáros, K. Murase, M. Mostafá and S. Coutu, [[arXiv:1809.09615](#)].
- [13] J. H. Collins, P. S. Bhupal Dev and Y. Sui, *Phys. Rev. D* **99** (2019) 043009 [[arXiv:1810.08479](#)].
- [14] L. Heurtier, Y. Mambrini and M. Pierre, *Phys. Rev. D* **100** (2019) 063011 [[arXiv:1902.04584](#)].
- [15] A. Abdul Halim et al. [Pierre Auger Coll.], accepted in *Phys. Rev. Lett.* 2025; see also E. De Vito [Pierre Auger Coll.], *PoS (ICRC 2023)* (2023) 1099.
- [16] V. Novotny [Pierre Auger], *PoS (ICRC 2019)* (2019) 374.
- [17] A. Aab *et al.* [Pierre Auger], *Phys. Rev. D* **102** (2020) 062005 [[arXiv:2008.06486](#)].
- [18] A. Abdul Halim et al. [Pierre Auger Coll.], publication in preparation (2023); see also M. Schimp [Pierre Auger Coll.], *PoS (ICRC 2021)* (2021) 968.